

Microwave absorption and bandwidth study of Y_2Co_{17} rare earth soft magnetic alloy with easy-plane anisotropy

Yun-Guo Ma(马云国), Liang Qiao(乔亮), Zu-Ying Zheng(郑祖应), Hong-Bo Hao(郝宏波), Hao Wang(王浩), Zhe Sun(孙哲), Cheng-Fa Tu(涂成发), Tao Wang(王涛), Zheng Yang(杨正), and Fa-Shen Li(李发伸)

Citation: Chin. Phys. B, 2023, 32 (**8**): 084202. DOI: 10.1088/1674-1056/aca148
Journal homepage: http://cpb.iphy.ac.cn; http://iopscience.iop.org/cpb

What follows is a list of articles you may be interested in

High-performance chiral all-optical OR logic gate based on topological edge states of valley photonic crystal

Xiaorong Wang(王晓蓉), Hongming Fei(费宏明), Han Lin(林瀚), Min Wu(武敏), Lijuan Kang(康丽娟), Mingda Zhang(张明达), Xin Liu(刘欣), Yibiao Yang(杨毅彪), and Liantuan Xiao(肖连团)

Chin. Phys. B, 2023, 32 (**7**): 074205. DOI: 10.1088/1674-1056/accb41

High efficiency and high transmission asymmetric polarization converter with chiral metasurface in visible and near-infrared region

Yuhang Gao(高雨航), Yu Tian(田宇), Qingguo Du(杜庆国), Yuanli Wang(王原丽), Qin Fu(付琴), Qiang Bian(卞强), Zhengying Li(李政颖), Shuai Feng(冯帅), and Fangfang Ren(任芳芳)

Chin. Phys. B, 2023, 32 (**7**): 074201. DOI: 10.1088/1674-1056/acb9eb

Theoretical research on the transverse spin of structured optical fields inside a waveguide

Zhiyong Wang(王智勇), Xiangru Wang(汪相如), Anran Li(李岸然), Kaiqiang Zhang(张开强), Yukun Ji(纪玉坤), and Mingyu Zhong(钟明玉)

Chin. Phys. B, 2023, 32 (**6**): 064207. DOI: 10.1088/1674-1056/acbf28

Synthesis, magnetic and electromagnetic wave absorption properties of planar anisotrop Y_2Co_{17}@SiO_2 rare earth soft magnetic composites

Liang Qiao(乔亮), Cheng-Fa Tu(涂成发), Wei Wu(吴伟), Wen-Biao Wang(王文彪), Sheng-Yu Yang(杨晟宇), Sun Zhe(孙哲), Peng Wu(吴鹏), Jin-Bo Yang(杨金波), Chang-Sheng Wang(王常生), Tao Wang(王涛), and Fa-Shen Li(李发伸)

Chin. Phys. B, 2023, 32 (**5**): 054202. DOI: 10.1088/1674-1056/aca7f1

Microwave absorption properties regulation and bandwidth formula of oriented $Y_2Fe_{17}N_{3-\delta}$@SiO_2/PU composite synthesized by reduction-diffusion method

Hao Wang(王浩), Liang Qiao(乔亮), Zu-Ying Zheng(郑祖应), Hong-Bo Hao(郝宏波), Tao Wang(王涛), Zheng Yang(杨正), and Fa-Shen Li(李发伸)

Chin. Phys. B, 2022, 31 (**11**): 114206. DOI: 10.1088/1674-1056/ac81ac

---

Microwave absorption and bandwidth study of Y_2Co_{17} rare earth soft magnetic alloy with easy-plane anisotropy

Yun-Guo Ma(马云国)[1], Liang Qiao(乔亮)[1,†], Zu-Ying Zheng(郑祖应)[1], Hong-Bo Hao(郝宏波)[2], Hao Wang(王浩)[1], Zhe Sun(孙哲)[1], Cheng-Fa Tu(涂成发)[1], Tao Wang(王涛)[1], Zheng Yang(杨正)[1], and Fa-Shen Li(李发伸)[1]

[1] *Institute of Applied Magnetism, Key Laboratory for Magnetism and Magnetic Materials of Ministry of Education, Lanzhou University, Lanzhou* 730000, *China*

[2] *State Key Laboratory of Baiyunobo Rare Earth Resource Researches and Comprehensive Utilization, Baotou* 014000, *China*

(Received 31 May 2022; revised manuscript received 7 November 2022; accepted manuscript online 9 November 2022)

The easy-plane anisotropy of the Y_2Co_{17} rare earth soft magnetic alloy has high saturation magnetization and operating frequency, and good impedance matching. Therefore, it is expected to become a kind of high-performance microwave absorbing material. In this paper, Y_2Co_{17} alloy was prepared by a reduction-diffusion method, and its micropowder was prepared as polyurethane (PU) based composite absorbing materials (Y_2Co_{17}/PU composites). The microwave properties of composites with different volume fractions were calculated. The composites showed outstanding absorption characteristics in the range of 20–30 vol%, and the minimum reflection loss (RL) was less than −50 dB. When the volume fraction was 25%, the effective absorption bandwidth could cover the X-band at a thickness of 1.5 mm, and the Ku-band at a thickness of 1.08 mm. The absorption mechanism was analyzed by the interface reflection model. The RL absorption peak bandwidth mechanism was discussed by using the amplitude relation and calculating the effective absorption bandwidth at different thicknesses. The effective absorption bandwidth values were in good agreement with the theoretical expectation.

Keywords: reduction-diffusion method, microwave absorption, interface reflection model, effective absorption bandwidth

PACS: 42.25.Bs, 42.81.Dp, 71.20.Eh, 72.30.+q **DOI:** 10.1088/1674-1056/aca148

1. Introduction

Microwave absorbing material was originally designed to be used in weapons and equipment to resist radar detection, for the purpose of stealth. With the rapid development of electronic information technology, the application of microwave absorbing materials is no longer limited to the military industry. In civil industries, microwave absorbing materials are widely used to solve the problems of electromagnetic pollution and interference caused by electronic equipment and electronic communication.[1–6]

Microwave absorbing materials can be classified as dielectric absorbing materials and magnetic absorbing materials. Compared with dielectric materials, it is easier to achieve impedance matching with magnetic materials, and their matching thickness is thinner, so they have become popular absorbing materials.[7–11] Due to the existence of Snoek's limit, the initial permeability and natural resonance frequency of the traditional axially magnetocrystalline anisotropic soft magnetic materials are mutually restricted, so they cannot have high permeability at high frequencies, which is not conducive to high frequency application. Magnetic materials with easy-plane magnetocrystalline anisotropy, due to "breakthrough" of Snoek's limit, can obtain high operating frequencies while still having high magnetic permeability, so they have greater potential in microwave absorption applications.[12–14]

As a soft magnetic alloy with easy-plane anisotropy, Y_2Co_{17} has high saturation magnetization, high working frequency and high permeability. It has been studied in the field of microwave absorption. He *et al.*[15] prepared Y_2Co_{17} by an arc melting method and studied its microwave absorbing properties. The results showed that Y_2Co_{17} has good low frequency absorption performance, with a minimum RL of −9.5 dB at 3.8 GHz. Zhong *et al.*[16] studied the absorbing performance of $Y_2Co_{17-x}Fe_x$ at high frequencies. The best absorbing performance was obtained when $x = 9$, the thickness was only 2 mm at the best matching, the minimum RL was −46.9 dB, and the effective absorption bandwidth was 4.74 GHz. At present, most of the preparation of Y_2Co_{17} is done using traditional processes such as smelting methods, and the preparation of Y_2Co_{17} by the reduction-diffusion method has basically not been reported. In this paper, a Y_2Co_{17} alloy was prepared using the reduction-diffusion method. The basic principle was that rare earth oxides were reduced to rare earth metals by reducing agent metals, and then rare earth soft magnetic alloys were directly prepared through the interdiffusion reaction of rare earth metals and 3d transition group magnetic metals. Compared with the traditional process, the reduction-diffusion method has the advantages of being a simple process, using cheap raw materials and a short preparation period. It has been applied well in the preparation of some magnetic materials.[17–23]

In this paper, Y_2Co_{17} was prepared using the reduction-

†Corresponding author. E-mail: qiaoliang@lzu.edu.cn

© 2023 Chinese Physical Society and IOP Publishing Ltd

diffusion method. The ball-milled powder was compounded with polyurethane (PU) to prepare Y_2Co_{17}/PU composite absorbing materials with different volume fractions. The microwave absorption properties of materials with different matching thicknesses were calculated. The microwave absorption mechanism of the composites was analyzed by using the interface reflection model, and a reasonable explanation for the appearance of the RL absorption peak was given. It also explains the influence of reflection factor and microwave refractive index on the absorbing properties of composite materials, which has important guiding significance for designing absorbing materials to reduce the RL and matching thickness. With a volume fraction of 25% composite absorbing material, when the thickness was 1.86 mm, the absorption peak frequency $f_m = 7.78$ GHz, the minimum $RL_{min} = -65.3$ dB and the effective absorption bandwidth (EBW, $RL < -10$ dB) was 2.73 GHz, it has the perfect matching. When the thickness of the absorber was 1.5 mm, its EBW could cover the X-band, and when the thickness of the absorber was 1.08 mm, its EBW could cover the Ku-band. In addition, the bandwidth under different thicknesses was calculated by the amplitude relationship, and the influencing factors of the bandwidth were discussed. The calculated values were in good agreement with those calculated by transmission line theory.

2. Experiment

The mass ratio of Y_2O_3, Co powder and Ca is given by the reaction equation

$$Y_2O_3 + 17Co + 3Ca = Y_2Co_{17} + 3CaO, \quad (1)$$

where Y_2O_3 and Ca should be excessive. The weighed raw materials were thoroughly mixed and pressed into a cake shape, and the original Y_2Co_{17} sample was prepared by reduction-diffusion reaction in an argon atmosphere. The prepared sample was crushed and screened with a 200-mesh sieve, and the residual CaO in the reaction process was washed away. Y_2Co_{17} powder was obtained after drying. The Y_2Co_{17} powder was ball milled by a planetary ball mill. Ball milling was performed at a speed of 200 rpm for 4 hours. The ball-milled Y_2Co_{17} magnetic powder was added to an acetone solution containing a certain amount of polyurethane, and was sonicated until the acetone was completely volatilized. After rotating orientation in a magnetic field, the composite was dried. Then, it was pressed into a ring-shaped composite material with an outer diameter of 7 mm and an inner diameter of 3.04 mm. The volume fractions of Y_2Co_{17} in the prepared composite samples were 15%, 20%, 25% and 30%, respectively.

X-ray diffraction (XRD) with Cu-$K\alpha$ radiation was used to characterize the crystal structure and phase composition of the Y_2Co_{17} magnetic powder. The morphology of the sample was characterized by scanning electron microscope (SEM), and the saturation magnetization (M_s) and coercivity (H_c) of the Y_2Co_{17} were measured by vibrating sample magnetometer (VSM). The complex permeability and complex permittivity of the composite magnetic ring in the frequency range of 0.1–18 GHz were measured using a vector network analyzer.

3. Results and discussion

3.1. Phase composition and morphological features

Figure 1 shows the XRD patterns of Y_2Co_{17} powder before and after ball milling. The Y_2Co_{17} prepared by the reduction-diffusion method has the rhombus structure of Th_2Zn_{17}-type. Its diffraction peak position and intensity can completely correspond to the standard Y_2Co_{17} sample pattern, with no impurity peak, and it has good crystallinity. It can be seen from the figure that the peak positions of the Y_2Co_{17} did not change before and after ball milling, and the matching degree is very good. Table 1 shows the lattice parameters of the samples before and after ball milling. After ball milling, the grain size decreased from 60.9 nm to 38.1 nm, lattice constants a and c increased slightly, but finally the c/a ratio decreased.

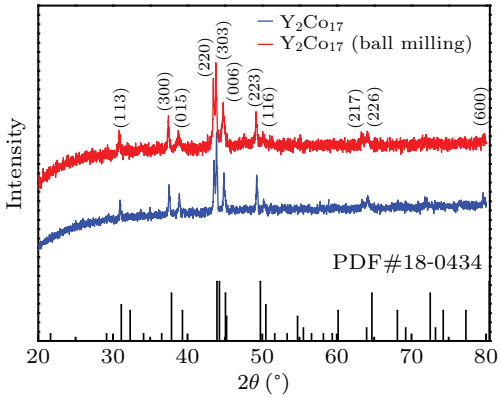


Fig. 1. XRD patterns of Y_2Co_{17} before and after ball milling.

Table 1. Lattice parameters of different samples, where δ is average grain size.

Sample	δ (nm)	a	c	c/a
Y_2Co_{17}	60.9	8.2626	12.1824	1.4744
Y_2Co_{17} (ball milling)	38.1	8.2882	12.2188	1.4742

The morphology of the Y_2Co_{17} powder before and after ball milling was characterized by scanning electron microscope (SEM), as shown in Fig. 2. Before ball milling, the average particle size of the sample is about 5–10 μm, showing an irregular shape. The average particle size of the sample is reduced to less than 5 μm by ball milling, and some particles have been ball-milled into flakes with a thickness of only 0.7 μm. After ball milling, the particle size of the sample is reduced. When the sample is made into a composite material,

PU can better cover the Y_2Co_{17} particles, the contact probability between particles is reduced, and the corresponding permittivity is greatly reduced. The permeability of the flaky samples decreased slowly, and its permeability after 1 GHz is greater than that of the irregular samples. High permeability and small permittivity are beneficial to impedance matching and improve absorption performance.[24]

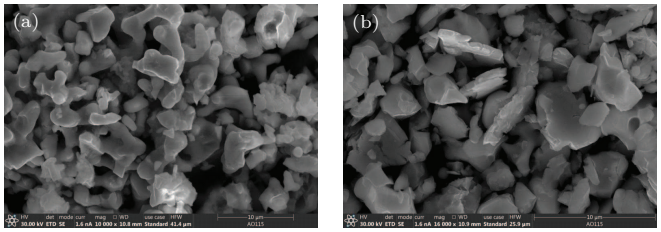


Fig. 2. (a) SEM image of unball-milled Y_2Co_{17} powder sample, (b) SEM image of ball-milled Y_2Co_{17} powder sample.

3.2. Static magnetic properties and degree of plane orientation

The static magnetic properties of the Y_2Co_{17} sample were characterized, and the hysteresis loop is shown in Fig. 3(a). The saturation magnetization before and after ball milling is 117 emu/g, which is almost unchanged. The coercivity increased from 54 Oe to 179 Oe. The increase of coercivity is attributed to the internal strain induced by the ball milling. The results show that Y_2Co_{17} not only has high saturation magnetization, but also has good soft magnetic properties.[25] In addition, the increase in coercivity can increase magnetic anisotropy, so that the resonance frequency moves to high frequencies, and the magnetic permeability is still high at high frequencies. Therefore, compared with the samples without ball milling, the ball milled samples have better high-frequency magnetic properties and microwave absorption properties.[26]

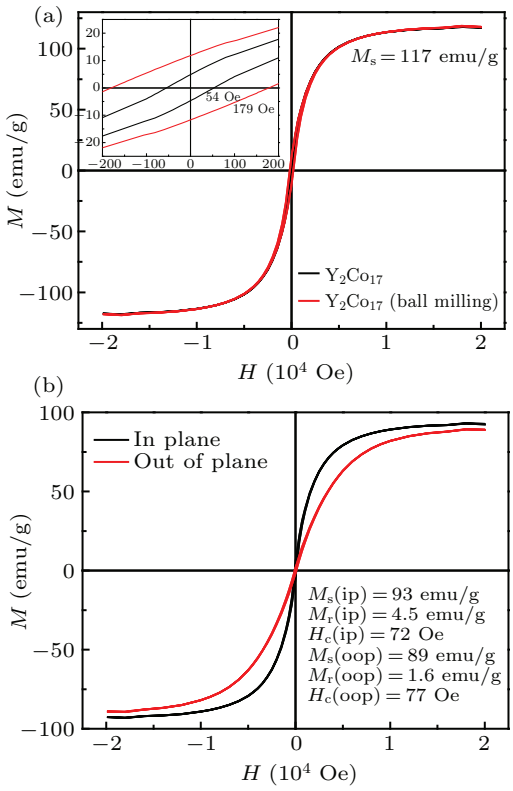


Fig. 3. (a) Magnetic hysteresis loops of Y_2Co_{17} powder before and after ball milling, (b) in-plane and out-of-plane hysteresis loops of Y_2Co_{17}/PU composites.

The degree of plane orientation (DPO) is an important parameter to determine whether a magnetic material has an easy-plane magnetocrystalline anisotropy. Its formula is[12]

$$\mathrm{DPO} = \frac{M_s - M_{r,z-\mathrm{axis}}}{M_s} \times 100\%. \tag{2}$$

The saturation magnetization M_s of Y_2Co_{17}/PU composites is 93 emu/g, which is determined by the in-plane hysteresis loop shown in Fig. 3(b), and the remanent magnetization $M_{r,z-\mathrm{axis}}$ in the z-axis direction is 1.6 emu/g, where the z-axis refers to the axis perpendicular to the easy plane. The degree of plane orientation calculated by formula (1) is 98.28%. It can be seen that the magnetic moment of Y_2Co_{17} is basically in the easy plane direction after orientation, and the distribution of magnetic moments along the z-axis is very small, indicating that the material has a good easy-plane property, that is, Y_2Co_{17} is a soft magnetic material with easy-plane anisotropy.

3.3. Electromagnetic parameters of Y_2Co_{17}/PU composites

Figure 4 shows the electromagnetic parameters of the Y_2Co_{17}/PU composites with different volume fractions (vol% = 15%, 20%, 25%, 30%). With the increase of the volume fraction of Y_2Co_{17}, the content of non-magnetic and electrically insulated polyurethane gradually decreases, leading to permeability and permittivity increases of the composites. When frequency is 0.1 GHz, the real part of the permeability increases from 1.9 to 3, and the real part of the permittivity increases from 10.4 to 23.6. Before the frequency of 0.3 GHz, the real part of the permeability of all samples remained unchanged, and in the frequency range of 0.3–18 GHz, the real part of the permeability decreases with the increase of frequency. This is mainly because of the magnetic resonance and the skin effect of magnetic particles at high frequencies. However, the permittivity (ε') has a very small decrease in the 0.1–18 GHz frequency range, indicating that the polarization relaxation phenomenon does not occur with the increase of frequency at high frequency, so it basically remains unchanged.[27] There are double resonance peaks in the imaginary part of the permeability, according to the mechanism of domain wall displacement and spin rotation. We know that there are only domain wall resonance and natural resonance in this frequency range; the former is a domain wall resonance peak and the latter is a natural resonance peak.[28]

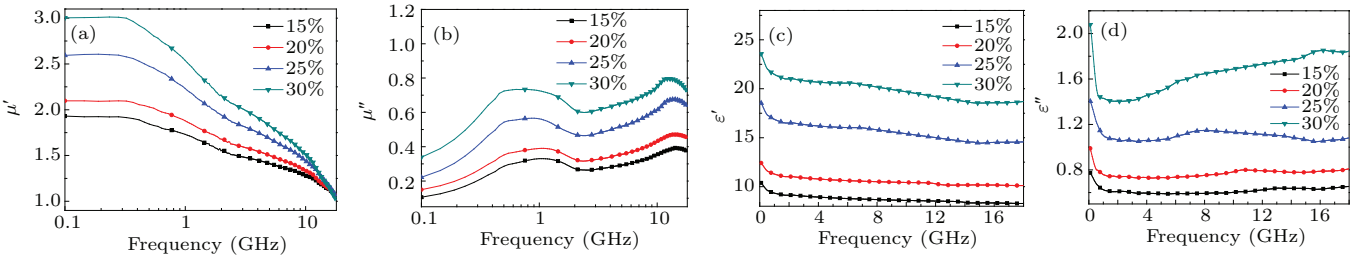
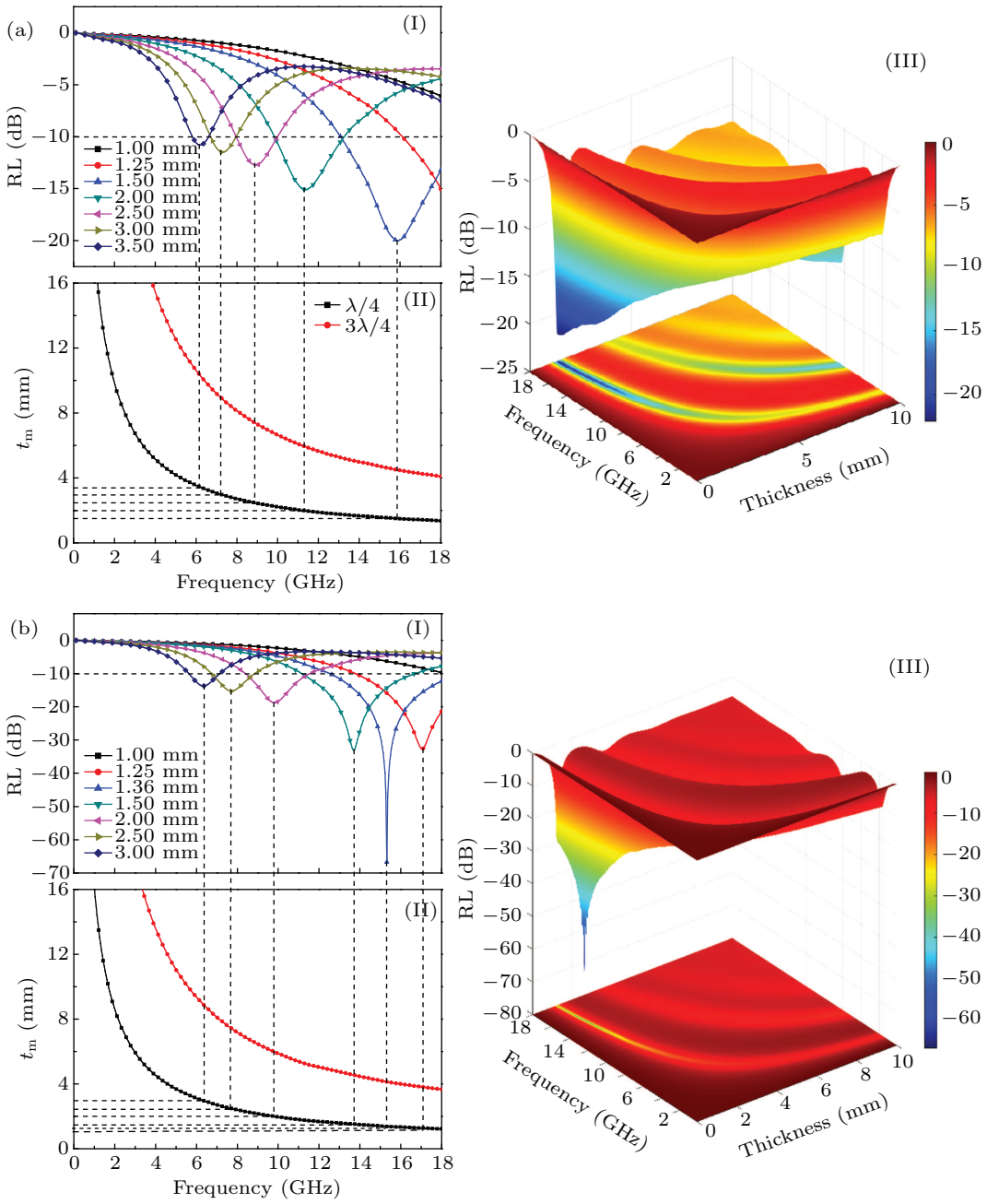


Fig. 4. Electromagnetic parameters of Y_2Co_{17}/PU composites with different volume fractions. (a) Real parts and (b) imaginary parts of the complex permeability, (c) real parts and (d) imaginary parts of the complex permittivity.

3.4. Reflection loss mechanism and microwave absorbing properties analysis of Y_2Co_{17}/PU composites

The main criteria to judge the microwave absorption performance of materials are the reflection loss (RL) of electromagnetic waves and the frequency width of RL < -10 dB, also known as the effective absorption bandwidth (EBW), which represents the frequency range that can absorb 90% of the energy of electromagnetic waves. Generally, at a given thickness, the smaller the RL, the wider the effective absorption bandwidth, and the better the absorption performance of the materials.



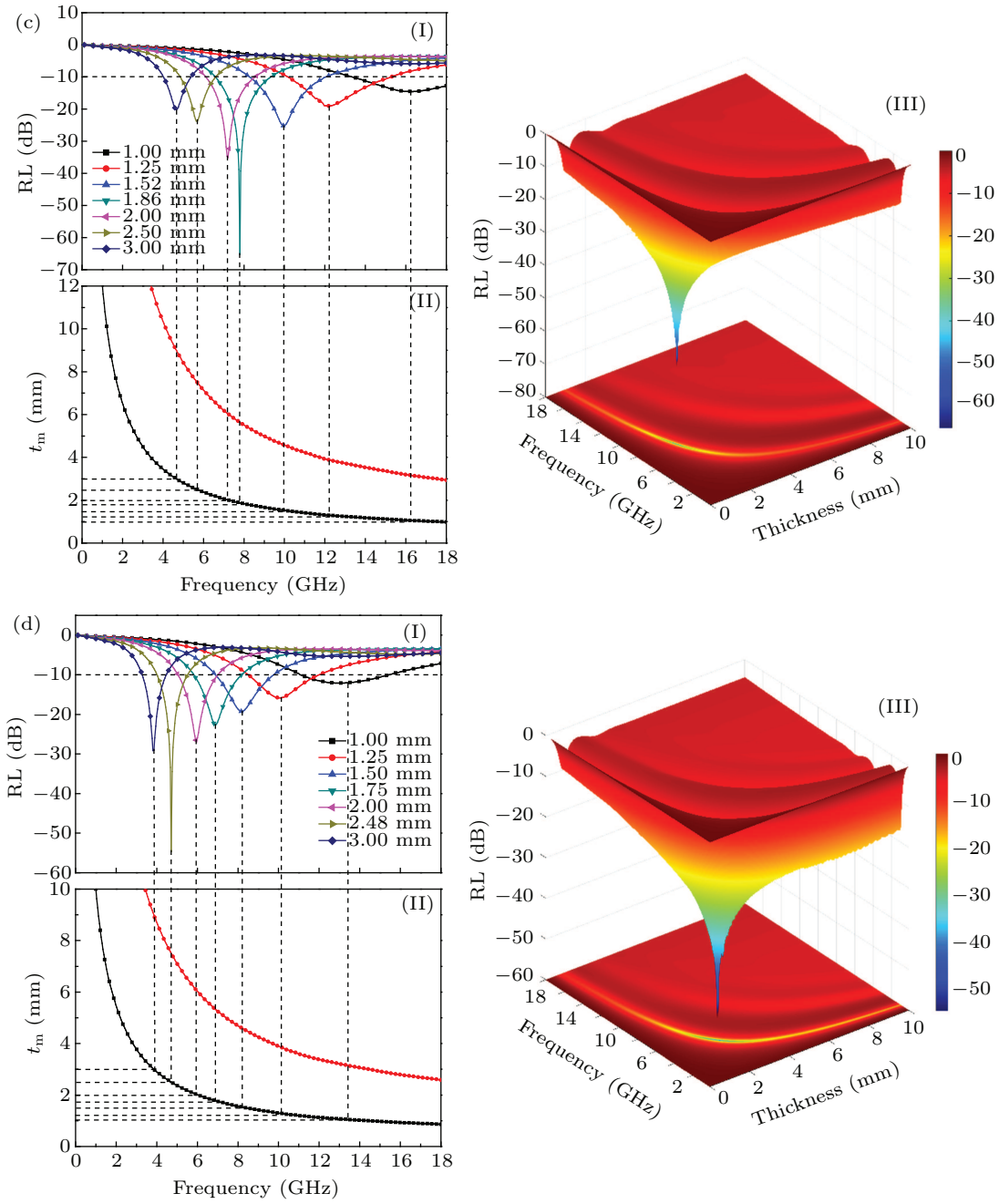


Fig. 5. RL curves and corresponding $\lambda/4$ and $3\lambda/4$ curves of Y_2Co_{17}/PU composites with different thicknesses, and three-dimensional RL graphs. (a) 15 vol%, (b) 20 vol%, (c) 25 vol%, (d) 30 vol%.

According to transmission line theory, the input impedance Z_{in} and the RL of the absorption material are calculated by the following equations:[29,30]

$$Z_{in} = Z_0\sqrt{\frac{\mu_r}{\varepsilon_r}}\tanh\left(j\frac{2\pi fd}{c}\sqrt{\mu_r\varepsilon_r}\right), \tag{3}$$

$$RL = 20\log_{10}\left|\frac{Z_{in}-Z_0}{Z_{in}+Z_0}\right|, \tag{4}$$

where Z_0 is the impedance of free space, μ_r and ε_r are the complex permeability and complex permittivity, respectively, f is the frequency of the electromagnetic wave, d is the thickness of the absorbing composites, and c is the velocity of light in a vacuum.

The RL of the Y_2Co_{17}/PU composite was calculated using the above the formulas, as shown in Fig. 5. Figures 5(a), (b), 5(c), and 5(d) are the microwave absorption characteristic curves of Y_2Co_{17}/PU composites with volume fractions of 15%, 20%, 25%, and 30%, respectively, where (I) is the RL graphs under different thicknesses, and (III) is the 3D graphs and sectional graphs of the RL.

For composites with 20%, 25% and 30% volume fractions, all of them have good microwave absorption performance. In this frequency range, with the decrease of the absorber thickness, the peak value of the RL decreases first and then increases. At a certain frequency, the peak of the

strongest RL will appear. The smaller the thickness of the absorber, the higher the peak frequency, and the wider the effective absorption bandwidth. The composite with a volume fraction of 15% shows poor absorbing properties in the entire frequency range. When the thickness decreases from 3.5 mm to 1 mm, the peak value of RL decreases, but it is not less than −20 dB. According to the above rules, it can be seen that the frequency of its strongest RL peak is higher than 18 GHz.

For the absorbing coating with metal backing, part of the incident electromagnetic wave is reflected at the front interface, and part of it enters the absorber, then continues to reflect at the rear interface (at the metal backing), and finally enters the air medium through the front interface. According to the interface reflection model,[31] when the thickness of the absorber is equal to an odd multiple of the quarter-wavelength ($\lambda/4$) of the electromagnetic wave, the phase angles of the electromagnetic wave reflected from the front interface and from the rear interface differ by 180°, and then the phases match. At this time, the two kinds of electromagnetic waves will produce destructive interference at the front interface, and the RL will have a minimum value, forming a strong absorption peak. The condition that the thickness of the absorber is equal to an odd multiple of $\lambda/4$ is[32]

$$t_{\mathrm{m}} = \frac{nc}{4f\sqrt{|\mu_{\mathrm{r}} \cdot \varepsilon_{\mathrm{r}}|}}, \quad (n = 1, 3, 5, \ldots). \tag{5}$$

Figures 5(a)-II, 5(b)-II, 5(c)-II, 5(d)-II show the corresponding relationship between the quarter-wavelength thickness and frequency of Y_2Co_{17}/PU composites with different volume fractions. The matching thickness of the RL calculated by transmission line theory can perfectly correspond to the 1/4 wavelength thickness at this peak frequency. The law that the thickness of the absorber decreases with the increase of frequency can be explained by the condition of quarter-wavelength destructive interference.

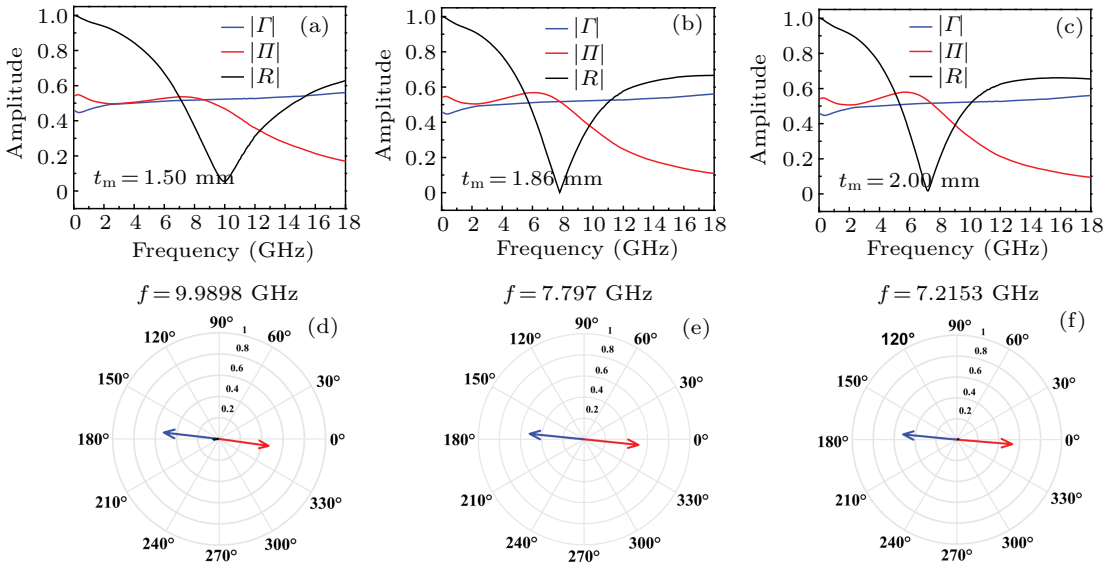


Fig. 6. (a)–(c) The relationship between Γ, Π, R and electromagnetic waves frequency, (d)–(f) the vector polar image when the sum of the reflection amplitudes is minimal.

Figures 6(a)–6(c) shows the relationship between the amplitude and frequency of the reflected wave at the front and rear interfaces after the electromagnetic wave passes through the Y_2Co_{17}/PU composite absorber with different thicknesses when the volume fraction is 25%. Figures 6(d)–6(f) show the vector polar image when the sum of the reflection amplitudes is minimal. The thickness of the absorber corresponding to (a) and (d) is 1.50 mm, to (b) and (e) is 1.86 mm, and to (c) and (f) is 2.00 mm. Γ represents the amplitude of the front interface reflection wave, Π represents the amplitude of the rear interface reflection wave, and R is the sum of the reflection amplitudes. The electromagnetic wave amplitude and energy have a square relationship. The smaller the sum of the electromagnetic wave amplitudes at the front interface is, the more energy the absorber absorbs, and the smaller the RL (the larger the absolute value). It can be seen from Fig. 6 that when the sum of the reflection amplitudes at different thicknesses reaches the minimum value, the phases of the reflected electromagnetic waves at the corresponding front and rear interfaces always differ by 180°. At this time, the amplitude values of reflected waves at the front and back interfaces are not necessarily equal. It shows that the RL has the minimum value, that is, the absorption peak is caused by the phase difference of 180° between the two electromagnetic waves. It is verified that the interface reflection model is used to explain the correctness of the RL peak.

Figure 7 shows the impedance matching diagram of the composites. It can be seen that when the input impedance of

the absorber is equal to the impedance of the free space, that is, when $Z_{in} = Z_0$, the RL peak shows the minimum value. According to Figs. 6(b) and 6(e), the two reflected electromagnetic waves not only have a 180° phase difference, but also have the same amplitude, so the electromagnetic waves are absorbed completely. The condition that the incident electromagnetic wave can be completely absorbed is called the perfect matching condition. It can also be seen from the figure that when the value of Z_{in}/Z_0 is closer to 1, the corresponding peak value of RL is smaller. This is also the reason why the RL decreases first and then increases with the matching thickness.

According to the interface reflection model, Table 2 lists the perfect matching conditions for composites with different volume fractions. It can be seen that with the increase of Y_2Co_{17} volume fraction, not only the frequency of electromagnetic wave is required for perfect matching decrease from 15.32 GHz to 4.71 GHz, but also the thickness of perfect matching becomes thicker and the EBW becomes smaller.

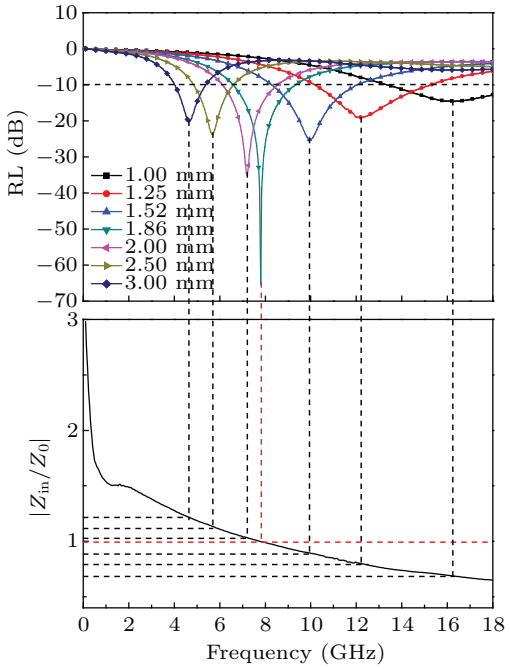


Fig. 7. Phase matching diagram of the Y_2Co_{17}/PU composite sample with a volume fraction of 25%. $Z_{in}/Z_0 = 1$ corresponds to the red line.

Table 2. Perfect matching conditions for composites with different volume fractions.

Volume fraction	Matching thickness (mm)	Frequency (GHz)	RL (dB)	EBW (GHz)
20%	1.36	15.32	–66.67	> 5.5
25%	1.86	7.8	–65.27	2.73
30%	2.48	4.71	–54.64	1.5

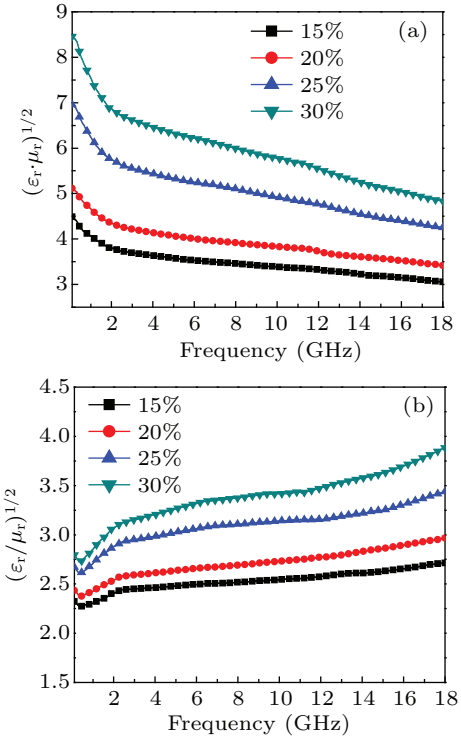


Fig. 8. (a) Microwave refractive index, (b) reflection factor.

According to formulas (3)–(5), the factors $\sqrt{|\mu_r/\varepsilon_r|}$ and $\sqrt{|\mu_r \cdot \varepsilon_r|}$ make important contributions to the absorption properties of composites, where $\sqrt{|\mu_r/\varepsilon_r|}$ is called the reflection factor and $\sqrt{|\mu_r \cdot \varepsilon_r|}$ is the microwave refractive index.

Figure 8 plots the reflection factor and microwave refractive index of Y_2Co_{17}/PU composites with different volume fractions. At a certain frequency, the microwave refractive index is inversely proportional to the matching thickness. It can be seen from Fig. 8(a) that increasing the volume fraction of the composite material can improve its microwave refractive index, so as to achieve the purpose of reducing the matching thickness. The absorption peak is caused by phase matching. At this time, the closer the amplitudes of the two reflected electromagnetic waves are, the smaller the RL. Therefore, in order to obtain good matching performance, the reflection amplitude of the front interface should be close to half of the incident electromagnetic wave amplitude. According to formula (5), the reflection amplitude of the front interface depends on the reflection factor, so the reflection factor can be used to adjust the value of the absorption peak.[31]

$$\Gamma = \frac{\sqrt{\mu_r/\varepsilon_r} - 1}{\sqrt{\mu_r/\varepsilon_r} + 1}. \tag{6}$$

In particular, for the composite with 25% volume fraction, when the thickness is 1.5 mm, its EBW almost completely covers the X-band; and when the thickness is 1.08 mm, its EBW completely covers the Ku band. It not only has a relatively thin matching thickness, but also has a very wide EBW at different thicknesses. As a microwave absorbing material, it conforms to the characteristics of "thin, light, wide

and strong", and is expected to be used as a good composite absorbing material in specific frequency bands.

In summary, at the same frequency, the volume fraction of the composites increases, and the microwave refractive index increases, which can make the matching thickness thinner. However, according to the change of RL in Fig. 5, the increase of the volume fraction will lead to a corresponding narrowing of EBW. And with the increase of Y_2Co_{17} content, the quality of the composite will also increase. Therefore, in order to obtain good absorption performance, the volume fraction of the prepared composites should be neither too low nor too high, and it must be considered comprehensively.

3.5. Bandwidth calculation

According to the interface reflection model, at a specific thickness, the reason for the RL absorption peak is that the phase difference of the electromagnetic waves reflected from the front and rear interfaces is π (180°) and destructive interference occurs. If the frequency of the incident electromagnetic wave changes and deviates from the matching peak frequency by a small value Δf, the corresponding electromagnetic wave phase angle will also change. The phase difference of the reflected waves at the front and rear interfaces becomes $\pi - \Delta\theta$, and the RL value becomes larger at this time. Using the amplitude relationship, the total amplitude of the electromagnetic wave at the absorption peak is[33]

$$A_0 = A_{\mathrm{fi}}\cos 0 + A_{\mathrm{ri}}\cos\pi = A_{\mathrm{fi}} - A_{\mathrm{ri}}, \tag{7}$$

where A_{fi} is the reflected electromagnetic wave amplitude at the front interface, and A_{ri} is the reflected amplitude at the rear interface. The total amplitude of the electromagnetic wave at a frequency Δf deviating from the absorption peak is

$$\begin{aligned} A_1 &= A_{\mathrm{fi}}\cos 0 + A_{\mathrm{ri}}\cos(\pi - \Delta\theta) \\ &= A_{\mathrm{fi}} - A_{\mathrm{ri}}\cos(\Delta\theta). \end{aligned} \tag{8}$$

Thus, the difference in the total amplitude at the two electromagnetic wave frequencies is

$$A_1 - A_0 = A_{\mathrm{ri}}[1 - \cos(\Delta\theta)]. \tag{9}$$

If $\Delta\theta \to 0$, then $\cos(\Delta\theta)$ can be expanded by Taylor's formula as

$$\cos(\Delta\theta) = 1 - \frac{(\Delta\theta)^2}{2} + o\left[(\Delta\theta)^2\right]. \tag{10}$$

Equation (8) can be simplified to get

$$A_1 - A_0 = A_{\mathrm{ri}} \cdot \frac{(\Delta\theta)^2}{2}. \tag{11}$$

$\Delta\theta$ and Δf have a mathematical relationship

$$\Delta\theta = \frac{\pi}{t_{\mathrm{m}}} \cdot \left[\left|\frac{\mathrm{d}t_{\mathrm{m}}}{\mathrm{d}f}\right| \cdot \Delta f\right]. \tag{12}$$

According to formulas (11) and (12), the bandwidth calculation formula is

$$\Delta = 2\Delta f = \left[\frac{2(A_1 - A_0)}{A_{\mathrm{ri}}}\right]^2 \cdot \frac{2t_{\mathrm{m}}}{\pi} \Big/ \left|\frac{\mathrm{d}t_{\mathrm{m}}}{\mathrm{d}f}\right|. \tag{13}$$

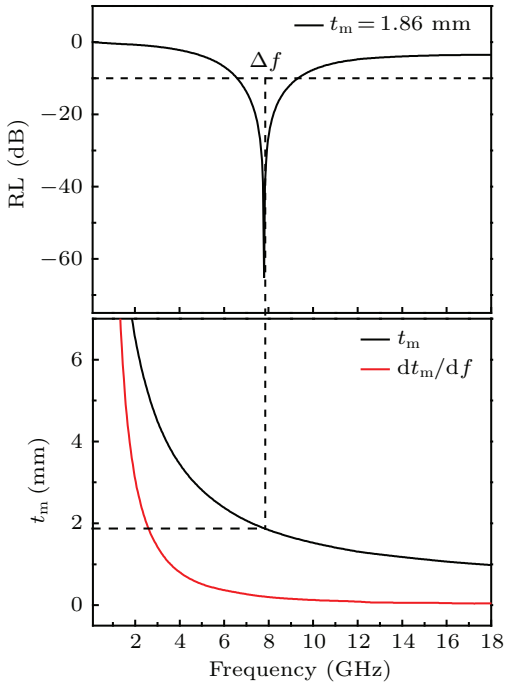


Fig. 9. Schematic diagram of the effective absorption bandwidth calculation.

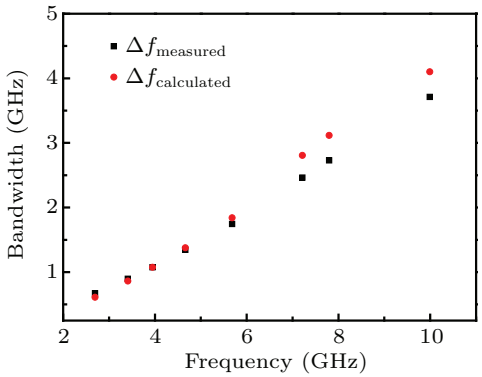


Fig. 10. Measured and calculated values of effective absorption bandwidth at different frequencies.

Using the above formula, the EBW of the Y_2Co_{17}/PU composites with 25% volume fraction was calculated. The calculated bandwidth value differs by a factor of 2 from the bandwidth value obtained by transmission line theory. This result is not only shown in the Y_2Co_{17}/PU composites in this paper, but the same result has also appeared in some magnetic and non-magnetic absorbing materials. Therefore, a 1/2 correction coefficient is introduced into the bandwidth formula, and the revised bandwidth calculation formula is obtained as

$$\Delta' = \frac{1}{2} \cdot \left[\frac{2(A_1 - A_0)}{A_{\mathrm{ri}}}\right]^2 \cdot \frac{2t_{\mathrm{m}}}{\pi} \Big/ \left|\frac{\mathrm{d}t_{\mathrm{m}}}{\mathrm{d}f}\right|. \tag{14}$$

Table 3. Parameters of the bandwidth formula and the comparison of theoretical and calculated values.

t_m (mm)	f_m (GHz)	$(RL)_{min}$ (dB)	A_{ri}	$\lvert dt_m/df \rvert$	$\Delta f_{measured}$	$\Delta f_{calculated}$	Relative error
1.50	9.99	–25.19	0.4692	0.1229	3.71	4.1	10.5%
1.86	7.80	–65.27	0.5178	0.2098	2.73	3.11	14.0%
2.00	7.22	–35.07	0.5313	0.2405	2.46	2.80	13.8%
2.50	5.69	–23.77	0.5708	0.4063	1.75	1.84	5.1%
3.00	4.66	–20.19	0.5993	0.5929	1.34	1.37	2.2%
3.50	3.95	–18.10	0.6225	0.8134	1.07	1.07	0%
4.00	3.41	–16.83	0.6405	1.0853	0.89	0.86	3.4%
5.00	2.70	-15.32	0.6631	1.7301	0.67	0.61	8.9%

Table 3 gives the relevant parameters for calculating the EBW under different thicknesses, and compares the values calculated using the modified bandwidth formula with the theoretical calculated values. The comparison results of the EBW at different frequencies are shown in Fig. 10. The results show that the error between the bandwidths calculated using the bandwidth formula and the theoretical calculation results is small, and the maximum relative error is less than 15%. This shows that the modified formula can be used to calculate the bandwidth of Y_2Co_{17}/PU composites.

4. Conclusion

In this work, an easy-plane anisotropic Y_2Co_{17} alloy was successfully prepared using a reduction-diffusion method, and the powder samples were ball-milled. SEM showed that part of the particles changed from irregular shape to flake shape after ball milling, which was beneficial to improve the microwave absorption performance. The electromagnetic parameters of Y_2Co_{17}/PU composites were discussed, the absorbing properties of composites with different volume fractions were analyzed, and the reflection loss and effective absorption bandwidth under different thicknesses were obtained. The microwave absorption mechanism of Y_2Co_{17}/PU composites was explained in detail by the interface reflection model. The effective absorption bandwidth of the composites was calculated by using the magnitude relationship, and the result was in good agreement with the expectation. In conclusion, Y_2Co_{17} is a promising microwave absorbing material.

Acknowledgements

Project supported by the National Key R&D Program of China (Grant No. 2021YFB3501302) and the National Natural Science Foundation of China (Grant No. 51731001). This work was also supported by the State Key Laboratory of Baiyunobo Rare Earth Resource Researches and Comprehensive Utilization's key of research and development projects.

References

[1] Liu X M, Xie G Z, Xie N Y, Gao X and Chen J 2020 *J. Mater. Sci.: Mater. Electron.* **31** 17502
[2] Luo J H, Xu Y and Gao D D 2014 *Solid State Sci.* **37** 40
[3] Wen F S, Zhang F, Xiang J Y, Hu W T, Yuan S J and Liu Z Y 2013 *J. Magn. Magn. Mater.* **343** 281
[4] Wang J W, Wang B B, Feng A L, Jia Z R and Wu G L 2020 *J. Alloys Compd.* **834** 155092
[5] Wang Y, He D W and Wang Y S 2021 *Chin. Phys. B* **30** 067804
[6] Huang H L, Xia H, Guo Z B, Chen Y and Li H J 2017 *Chin. Phys. B* **26** 025207
[7] Wang B L, Wu Q, Fu Y G and Liu T 2021 *J. Mater. Sci. Technol.* **86** 91
[8] Sista K S, Dwarapudi S, Kumar D, Sinha G R and Moon A P 2021 *J. Alloys Compd.* **853** 157251
[9] Liu Y, Li R, Jia Y and He Z X 2020 *Chin. Phys. B* **29** 067701
[10] Wang Y K, Lin Z C, Liu Z, Qiao G Y, Zhang P Y, Li K W, Yang W Y, Han J Z, Liu S Q, Wang C S, Qiao L and Yang J B 2022 *IEEE Trans. Magn.* **58** 2800204
[11] Zhuang X H, Tan G G, Ning M Q, Qi C Y, Ge X J, Yang Z and Man Q K 2021 *J. Alloys Compd.* **883** 160835
[12] Wu P, Zhang Y D, Hao H B, Qiao L, Liu X, Wang T and Li F S 2022 *J. Magn. Magn. Mater.* **549** 168962
[13] Hu Q W, Qiao G Y, Yang W Y, Liu Z, Zhang P Y, Liu S Q, Wang C S, Zhou D, Han R, Cai D Y, Hu B P and Yang J B 2020 *J. Phys. D: Appl. Phys.* **53** 115001
[14] Wang P, Wang X M, Qiao L, Zhang J M, Wang G W, Duan B F, Wang T and Li F S 2018 *J. Magn. Magn. Mater.* **468** 193
[15] He C K, Pan S K, Cheng L C, Liu X and Wu Y J 2015 *J. Rare Earths.* **33** 271
[16] Zhong J P, Tan G G, Man Q K, Ning M Q, Gao Y, Liu X C and Pan J 2021 *J. Mater. Sci.: Mater. Electron.* **32** 27849
[17] Yun J C, Jung S S, Lee J G, Choi C J and Lee J S 2010 *Mater. Sci. Forum.* **638–642** 1796
[18] Chang W K, Young H K, Hyun G C and Young S K 2006 *IEEE Nanotechnol. Mater. Devices Conf.* OCT 22–25, 2006 Gyeongju, SOUTH KOREA, p. 658
[19] Krishnan T S 1980 *Bull. Mater. Sci.* **2** 161
[20] Qi G J, Hino M and Yazawa A 1990 *Mater. Trans., JIM.* **31** 463
[21] Eom N S A, Jeon E J, Haq M A, Lee J M, Choa Y H and Kim B S 2020 *Mater. Lett.* **268** 127611
[22] Wang Y, Ahn J, Kim D, Ren W J, Liu W, Zhang Z D and Choi C J 2017 *J. Magn. Magn. Mater.* **439** 91
[23] Tian S J 2020 *Study on Preparation of Ultrafine Sm2Fe17N3 Magnetic Powder by reduction diffusion Method* (Master Dissertation) (Zhejiang: Zhejiang University of Technology)
[24] He Y, Pan S K, Cheng L C, Luo J L and Yu J J 2019 *J. Electron. Mater.* **48** 1574
[25] Wang T, Wei J Q, Zhang Z Q and Li F S 2013 *Mater. Chin.* **32** 94
[26] Liu X M, Xie G Z, Xie N Y, Gao X, Chen J 2020 *J. Mater. Sci.: Mater. Electron.* **31** 17502
[27] Wang G W, Zhang J M, Wang P, Wang T and Li F S 2020 *J. Magn. Mater. Devices.* **51** 5
[28] Wang P, Zhang J M, Wang G W, Duan B F, Wang T and Li F S 2020 *Appl. Phys. Lett.* **116** 112403
[29] Qiao L, Wen F S, Wei J Q, Wang J B and Li F S 2008 *J. Appl. Phys.* **103** 063903
[30] Zuo W L, Qiao L, Chi X, Wang T and Li F S 2011 *J. Alloys Compd.* **509** 6359
[31] Wang T, Zhang J M, Wang P, Qiao L, Tang L Y, Xie D S and Li F S 2016 *J. Magn. Mater. Devices* **47** 7
[32] Wang T, Wang H D, Tan G G, Wang L and Qiao L 2015 *IEEE Trans. Magn.* **51** 2800405
[33] Wang T, Han R, Tan G G, Wei J Q, Qiao L and Li F S 2012 *J. Appl. Phys.* **112** 104903